SMU Data Science Review

Volume 2 | Number 1 Article 4

2019

Application of Machine Learning in Satellite Derived Bathymetry and Coastline Detection

Kevin Dickens
Southern Methodist University, kalyndal@yahoo.com

Albert Armstrong
NGA, Albert.E.Armstrong@nga.mil

Application of Machine Learning in Satellite Derived Bathymetry and Coastline Detection

Kevin Dickens[1], Albert Armstrong[2]

[1] Master of Science in Data Science,
Southern Methodist University,
Dallas, TX 75275 USA
[2] National Geospatial-Intelligence Agency (NGA), 7500 GEOINT Dr,
Springfield VA 22150 USA
kdickens@smu.edu
Albert.E.Armstrong@nga.mil

Abstract. This study examines the use of a machine learning framework for predicting seafloor depth and coastline. The world's oceans obscure the majority of the Earth's surface, and due to continual tidal motion, currents, and natural events, the seafloor changes constantly. The world's oceans remain largely unsurveyed by modern technologies such as multi-beam sonar or are under-surveyed using antiquated techniques like lead-line. The increased availability and access of commercial imagery allows for the accurate prediction of bathymetric depths and the identification of coastline. DeepUNet is a sea-land segmentation deep learning model utilized to detect coastline. This study will modify the existing DeepUNet structure and preprocess the data using different techniques to ncrease accuracy of coastline detection. A Recurrent Neural Network (RNN)will then be utilized against preprocessed data in order to predict depths and then compared to an interpolated seafloor generated from nautical charting data. The results of this study indicate that derived bathymetry using deep learning techniques do not meet the International Hydrographic Organization (IHO) standards for inclusion in Safety of Navigation products. However, both tools allow the evaluation of areas in need of hydrographic surveying.

1 Introduction

Maritime commerce accounts for 90%[1] of all global trade yet detailed data exist for less than 5% of the ocean seafloor.[2] Navigating oceans is unlike via land or air as the dangers lie obscured to the operators of the vessel. Underwater hazards comprise

[1] International Chamber of Shipping. Shipping and World Trade. [Online.] http://www.ics-shipping.org/shipping-facts/shipping-and-world-trade [Accessed 28 October 2018]
[2] Seafloor Mapping: The Foundation for Healthy Oceans and a Healthy Planet. How Much of the Seafloor is Left to Explore? [Online.] https://oceanexplorer.noaa.gov/world-oceans-day-2015/how-much-of-the-seafloor-is-left-to-explore.html [Accessed 28 October 2018]

the most dangerous features for vessels in transit. If they remain uncharted, the navigation crew possesses few tools to detect them [1]. Hazards only appear on navigational products if reported, surveyed, or struck. Countries maintain few surveying vessels[3], and those that do only survey domestic waters leaving vast areas lacking modern survey data. Much of the world relies on older methods for sounding measurement such as single beam sonar and lead line which lack the granularity of modern survey techniques. Changing coastlines affects many aspects of human and natural life ranging from political, such as changing boundaries, humanitarian such as post-disaster cleanup, to ecological impacts - such as fisheries and receding coastline.

Bathymetry is simply the depth measurement from some vertical plane to the bottom of the seafloor. The vertical plane is usually set by a vertical datum. The International Hydrographic Organization (IHO) defines satellite derived bathymetry as "depths processed from optical satellite imagery".[4] Satellite derived bathymetry was first conceived in the 1970s [8]. The recent increase of highly available, high resolution data allows for more analysis and more robust and verifiable results. The basic premise of derived bathymetry focuses on shallow water appearing lighter in color than deeper water. Using multispectral imagery, or imagery collected with multiple electromagnetic bands of light, the bands can be evaluated to determine areas of higher reflected sunlight intensity [8]. The United Kingdom Hydrographic Office (UKHO) does not presently consider derived bathymetry data suitable for inclusion in maritime safety of navigation charting products [2]. However, derived bathymetry could be utilized to highlight areas of potential new bathymetric surveys.

Coastline accounts for tidal changes and, as such, coastline is typically collected at the highest astronomical tide level or the mean highest high-water level. These are averages of the highest water levels over a set period. The HAT83 vertical datum is tied to highest astronomical tide and sometimes appears as a vertical reference for coastline measurements [4].

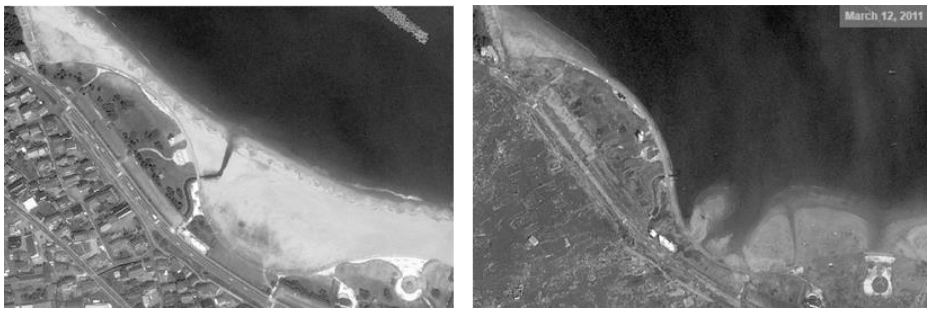

Figure 1. Coastline Before (left) and After (right) 2011 Japanese Tsunami

[3] Hydro-International. Ocean Survey – The World Market. [Online.] https://www.hydro-international.com/content/article/ocean-survey-the-world-market [Accessed 28 October 2018]

[4] International Hydrographic Organization. Satellite Derived Bathymetry. [Online] https://www.iho.int/mtg_docs/com_wg/CSPCWG/CSPCWG11-NCWG1/CSPCWG11-08.7A-Satellite%20Bathymetry.pdf [Accessed 24 October 2018]

Coastlines are more prone to change than many other environments due to the constant tidal forces at play. Natural disasters such as earthquakes, tsunamis, hurricanes, and typhoons exacerbate the already harsh tidal forces and can rapidly reshape coastlines [4]. The tsunami that hit Sumatra in 2004 left large segments of coastline altered.[5] The earthquake and resulting tsunami off Fukushima prefecture of Japan in 2011 shifted the entire island of Japan as much as 5m and dramatically altered the coastline along the eastern seaboard[6] as shown in Figure 1.

The use of derived bathymetry and detection of coastline from satellite imagery allows the producers of global navigational data to quickly add or update data on existing nautical charts. The added information keeps mariners safe from harm and increases awareness of potential hazards. The use of imagery to detect coastline can highlight the impact of natural disasters, reflect changes to political and administrative boundaries, and allow for better humanitarian relief. Automated and remote methods allow for the evaluation of large areas and focus survey resources to areas showing the large coastal changes or potential hazards to navigation.

2 Background

2.1 Bathymetric Survey Techniques

The predominant technique of modern bathymetric surveys is the utilization of multibeam sonar arrays. Modern bathymetric surveys utilize multibeam sonar arrays towed behind the survey vessel. Side-scan sonar is frequently utilized in addition to the multibeam sonar to better visualize a 3-dimensional surface and to aid in identifying objects and hazards on the seafloor [12]. Multi-beam sonar works by emitting a soundwave across a broad area and waiting for the return wave back. Once corrected for water properties an accurate depth is established. Multibeam sonar differs from older single beam sonar by broadcasting over a larger area. The track lines navigated by the survey vessels are broader and gaps between tracks appear less frequently as a result. In addition to depths, surveys measure other features such as salinity, turbidity, and temperature. These measurements will aid in the post-processing of the survey data as many factors affect the speed sonar travels through water. If performed near shore, a survey of nearby coastline could also be performed to update existing coastline records [12]. The result of a bathymetric survey generates a three-dimensional surface depicting the seafloor and containing depth information as well as multiple reports highlighting hazards, objects, and navigational aids in the surveyed area [12].

[5] University of Vermont. Coastline Changes to Aceh from the Great 2004 Sumatra-Andaman Earthquake. [Online] https://serc.carleton.edu/vignettes/collection/25462.html [Accessed 08 November 208]

[6] Physics Today. Insights from the Great 2011 Japan Earthquake. [Online] https://authors.library.caltech.edu/28770/1/Lay2011p16763Phys_Today.pdf [Accessed 05 November 2018]

Table 1. IHO S-44 Survey Categories and Standards

Order	1a	1b	2
Maximum allowable THU 95% Confidence level	5 meters + 5% of depth	5 meters + 5% of depth	20 meters + 10% of depth
Maximum allowable TVU 95% Confidence level	a = 0.5 meter b = 0.013 meter	a = 0.5 meter b = 0.013 meter	a = 1.0 meter b = 0.023 meter
Full Sea floor Search	Required	Not Required	Not Required
Feature Detection	cubic features > 2 meters, in depths up to 40 meters; 10% of depth beyond 40 meters	Not Applicable	Not Applicable
Maximum Line Spacing	Not defined as full sea floor search is required	3x average depth or 25 meters, whichever is greater For bathymetric lidar a spot spacing of 5 x 5 meters	4 x average depth
Positioning of fixed aids to navigation and topography significant to navigation (95% Confidence Level)	2 meters	2 meters	5 meters
Positioning of Coastline and topography less significant to navigation (95% Confidence Level)	20 meters	20 meters	20 meters
Mean Position of floating Aids to navigation (95% Confidence Level)	10 meters	10 meters	20 meters

Modern bathymetric surveys follow guidelines outlined in the S-44 standards and of the International Hydrographic Organization and shown in Table 1 [12]. These standards discuss the methods and procedures for conducting a bathymetric survey. Several orders of survey exist that determine the minimum accuracy and spacing between depth measurements of the survey data. A 1A survey is necessary for most shallow water areas frequently transited by large vessels [12]. Hydrographic offices conduct surveys around the world, but survey resources are limited and prone to political and natural disruptions. When planning surveys in foreign waters, a hydrographic office must obtain permission of the host country whose waters will be surveyed. This usually involves data sharing agreements and non-disclosure agreements to prevent commercial sale of the data. Once permission is granted, a survey team will plan and conduct the actual survey [12].

2.2 Remotely Sensed Data

Remotely sensed data consists of sensor data collected via a remote platform such as a satellite or plane. This data usually takes the form of a raster datatype comprised of many individual pixels that contain the sensor measurements. Typically, this data comes in the form of electromagnetic measurements collected at regular intervals and pieced together into images.[7] Collection sensors consist of measurements across a broad spectrum of the electromagnetic spectrum. Visible light, infrared, ultraviolet, microwave and radio waves are all examples of different bands

[7] BC Open Textbooks. Nature of Geographic Information Chapter 8 – Remotely Sensed Image Data. [Online] https://opentextbc.ca/natureofgeographicinformation/chapter/1-overview-7/ [Accessed 30 October 2018]

of electromagnetic radiation. [13]

Multispectral imagery can be utilized for a broad range of analysis by manipulating the individual bandwidths of electromagnetic radiation[4]. Everything reflects or emits EM radiation and exhibits different spectral response patterns. By measuring an individual objects spectral response pattern, the different bands can be utilized to highlight reflectivity or emission of specific bands. Thus, band manipulation can aid in identifying specific materials, vegetation, or the presence of water.

The data in those pixels are constrained by the sensors of the platform. The capability of the remote sensors is defined by the spatial, spectral, and radiometric resolution[4]. Spatial resolution measures the geographic area an individual pixel covers. Resolution varies widely across platforms with the best resolutions only 1 square meter all the way up to resolutions kilometers in size. Spatial resolution affects the granularity of what features can be detected. If a single pixel measures 30 square meters, then a small house measuring 15 square meters will not show up on the image. Radiometric resolution measures the precision of the sensor for a specific electromagnetic band[4]. EM radiation moves in waves thus the radiometric resolution measures the area under the wave. The more bytes allocated to a pixel for a specific EM range, the greater the radiometric resolution. Spectral resolution by comparison measures the sensors ability to detect small changes in wavelength. Thus, spectral resolution determines the minimum threshold for change to the height of the wave that the sensor can detect. [13]

2.3 Derived Bathymetry Techniques

In contrast to the techniques described previously, which take direct measurements from survey vessels, derived bathymetry from remotely sensed data relies heavily on understanding and adjusting for the physical properties of water, the seafloor, and the atmosphere. Water conditions vary widely at small and large scales which must be accounted for in the interpretation of Imagery. The variance of physical properties of seafloor materials can also affect interpretation of imagery. Likewise, the seafloor is comprised of many different materials and each of those materials exhibit their own physical properties which can affect interpretation of imagery. The atmosphere plays a role in affecting the interpretation of imagery. All these factors must be accounted for when deriving depths from remotely sensed data. [9]

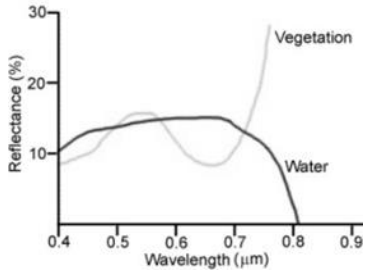

Figure 2. Spectral Reflectivity of Water vs. Vegetation

How water reflects and absorbs EM radiation, plays a large role in derived bathymetry techniques. The primary property examined by derived bathymetry is the reflectivity of EM bands. Water reflects each band at varying rates and measuring this reflectivity allows for prediction of depth. This is not without complications. Figure 2 shows the reflectivity of water and vegetation where vegetation exhibits lower spectral reflectance at most wavelengths than vegetation. This means that the near infrared bands will not penetrate water beyond a depth of 1-2 feet, while the lower wavelengths will travel deeper. When the angle of the sensor and the solar angle interact with water's natural reflectivity, sun-glint may occur. Sun-glint is light reflected directly back at the sensor that shows up as a glare [8]. Additionally, many other factors affect into the reflectivity of water such as turbidity and salinity. Turbidity measures the particulate matter in the water and high turbidity can lead to increased reflectivity. Salinity measures the salt content of the water and can also affect the reflectivity and the speed at which EMR travels through water. Both measures affect overall water clarity. [12]

Many different materials comprise the seafloor in each area, and these can vary within a short distance. Coral, sand, rocks, and mud are all examples of different bottom materials of the seafloor. Each material has their own physical properties including how they reflect different bands of EM. Some of these materials can greatly impact the clarity of the water as well [9].

Any attempts to derive depths or characteristics from remotely sensed imagery must adjust for atmospheric interference. The atmosphere reflects some of the EM bands algorithms must adjust for this loss. Clouds prevent collection of data over areas and provide a confounding element if not adjusted for by either removing pixels of suspected clouds or otherwise correcting by using other bands such as Near Infrared that can more readily penetrate clouds [3].

The foundation of derived bathymetry stems from two well established algorithm models by Lyzenga and Stumpf. Both provide prediction capabilities where error increases in deeper water. At depths greater than 40 meters the models become unreliable.

The Lyzenga model uses multiple algorithms for depth determination from imagery. Chief among these algorithms is the depth-estimation algorithm that factors in the other algorithms that correct for sun-glint and uses the reflectance model to determine deep-water signal correction [8]. The weakness of the model comes from variations of bottom reflectance that are unaccounted for although these can be mitigated using multiple spectral bands [8].

Stumpf developed an algorithm for deriving bathymetric depths from remotely sensed imagery that allows for different reflectance of bottom materials [9]. The Stumpf model consists of two parts: a linear model and a ratio model. The Stumpf model also allows for training to be introduced using existing sounding data [9].

2.4 Coastline Extraction Techniques

In imagery, the boundary between land and water is easy to detect using traditional methods such as histogram thresholding or equalization. Any approach for coastline detection must account for several factors including atmospheric interference, differing coastline materials, and tidal influences [5]. Equalization shifts colors in pixels to equal frequency across the image. The result increases the

contrast of the image and exaggerates differences between light and dark sections of the image [10]. Histogram thresholding is an iterative process that reduces each pixel to a binary black/white for even greater exaggeration. The iterative nature weighs the histogram in each successive processing of the image and binning values as lighter or darker [10]. Figure 3 shows an example of both equalization and thresholding.

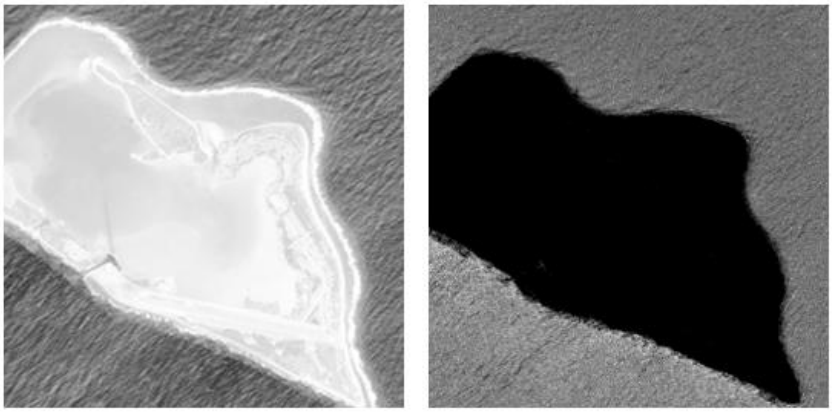

Figure 3. Example of Equalization and Histogram Thresholding

This paper uses a deep learning model that effectively classifies each pixel as a binary like thresholding with edge detection filters to increase the accuracy of the extracted coastline [10]. Edge detection is used to extract edges between pixel edges. The process is useful for creating linear features such as coastlines. The blur filter is a common method to reduced noise and allows for greater contrast and easing the processing requirements of later steps. Histogram thresholding then creates a segmented image where the binary elements represent water and land [10].

2.5 Deep Learning Techniques

Deep learning is a machine learning discipline that involves the creation and implementation of large neural networks and typically involves large amounts of data with more complex models. These deep networks benefit from increased scale via feature learning which allows these networks to self-correct. Neural networks are not a new concept and a great deal of research has occurred on this topic in the past 70 years[8]. Neural networks attempt to simulate the way a brain works by replicating dense interconnected nodes to aid in problems of pattern recognition and decision making.

Neural networks consist of many nodes, referred to as neurons, or units, arranged in a series of layers as shown in Figure 3. Each layer contains connections to the previous layer and to a further layer. On one side, the input neurons receive data for analysis. This starts the process of learning. At the end of the network are the output neurons which relay the results of analysis [11]. In between the input and the

[8] MIT News. Explained: Neural Networks. [Online] http://news.mit.edu/2017/explained-neural-networks-deep-learning-0414 [Accessed 4 November 2018]

output neurons are a series of neurons referred to as hidden neurons which form the bulk of the network. Connections between nodes and layers are represented numerically and referred to as a weight. A positive weight means that a connection is beneficial while a negative weight indicates an inhibitive relationship between the two nodes. [11]

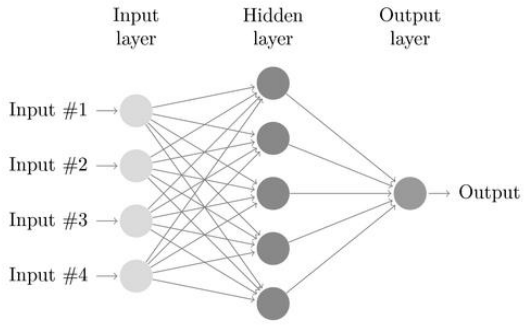

Figure 4. Basic Neural Network Architecture

Information can flow through the network in two ways. Feedforward or backpropagation. Feedforward refers to data flowing through a network in only a single direction. The input nodes will take the data and feed it to the next layer. Each layer passes the data onto the next layer until the resulting data ends up in the output nodes [11]. Not all neurons transmit data to the next node, however. Inputs are multiplied by the weights and must meet a threshold in order to be passed to new nodes. Backpropagation creates a feedback element for neural networks. This takes the actual output and compares it to the expected output and uses the difference between them to modify the weights of the connections [11]. In this manner, the weights of the edges continue to be re-calculated as new data comes in. Eventually, the edge weights will stabilize once the neural network processes enough training data. [11]

Neural Networks find uses in many places. Much of their use focuses on simple decision making or feature classification and extraction. Due to the iterative process and feedback propagation, neural networks are ideal for pattern detection, which is a form of classification. Given enough training data, a neural network can eventually distinguish elements of images such as a dog or cat. In this study neural networks will be used to detect areas of shallow water and land-water boundary. [11]

2.6 Neural Network Types and Structures

Many different types of neural networks exist from simple artificial neural networks (ANN), to more complex networks, including convolutional neural networks (CNN), generative adversarial networks (GAN), and recurrent neural networks (RNN). The list of neural network types continues to expand with time as researchers develop new methods to address certain issues and topics [11]. Many of

these neural network types utilize the same components within their structures, but either layer or organize them differently.

A simple ANN, shown in figure 4, also called a perceptron, consists of a series of inputs, hidden nodes, and outputs. All nodes are fully connected, and activation moves from an input to an output without any back propagation. For simple ANNs there is only ever a single hidden node layer between the input and output. [11]

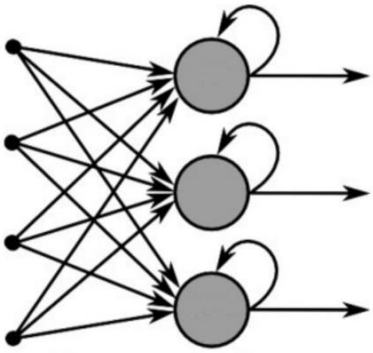

Figure 5. Basic Recurrent Neural Network Architecture

Recurrent neural networks, like the one shown in figure 5, take the input and output nodes of an ANN and connect them with a new node type, recurrent nodes. These recurrent nodes are also called context sensitive nodes because they consider the decisions of past iterations. These past iterative states influence the current decision. In this case RNNs are extremely useful for ordered data and time-series analysis.

Convolutional neural networks use convolutional layers to operate on three-dimensional data such as images. CNNs use a sliding frame that processes a small subset of the input image at a time. This frame moves along the image and processes the image by using the convolutional layers to simplify the image section by removing unnecessary information. As the frame moves along it can also up-sample the existing section to add detail and recreate an image. CNNs are usually used for image recognition and feature detection [11].

2.7 DeepUNet Structure

DeepUNet was developed as a symmetrical and sequential network with recurrent plus connections built into the structure to treat an image as ordered data. The basic structure of DeepUNet consists of a convolutional block designed to use the RGB channels of remotely sensed imagery and output binary feature maps as shown in Figure 5. The network does not utilize fully connected layers but rather a series of sequential convolutional blocks strung together. These blocks work to both deconstruct and simplify the image to produce ideal results and then reconstruct a suitable output. These convolutional blocks are also connected via plus connections that pass the input of the previous block to the next block. In this way DeepUNet

can consider the context in the current process. At the end of the network is a SoftMax layer that produces the final segmentation map with the binary output. [20]

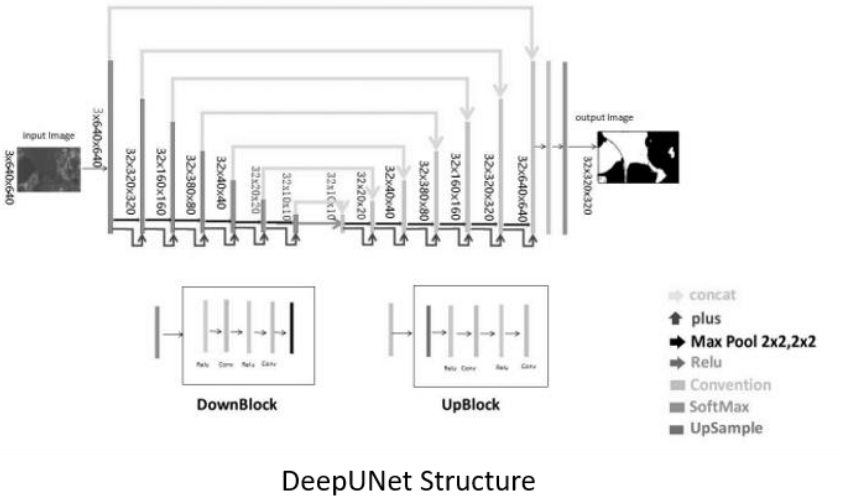

Figure 6. DeepUNet Structure implemented by Ruirui Li et al [20]

The convolutional blocks in DeepUNet serve two purposes as mentioned previously. They either down sample the RBG channels and make predictions or they up sample to produce an optimal output. These convolutional blocks consist of a series of layers as shown in Figure 6. In the early stages of the network the convolutional blocks consist exclusively of DownBlocks. Each DownBlock consists of a series of convolutional nodes which pass along the activation function, in this case a rectified linear unit (ReLu). ReLu layers are commonly used as activation layers after linear operations to introduce non-linearaity. In the past tanh and sigmoid were used but ReLu offers greater computational efficiency. At the end of each block the output is passed via a maxpooling layer with 2x2 kernel and step size. The downblocks follow several iterations growing successively courser in block size starting at 320x320 and ending up with 10x10 block before sending to the UpBlocks.[20]

After ideal results are passed from the DownBlocks, the UpBlocks begin rebuilding the original structure of the image with the optimal results. The UpBlocks follow a symmetry to the DownBlocks where they start at 10x10 pixel size and finish with 640x640 pixels, the size of the original input. The DownBlocks are similar in structure as well except they use an upsample node in the front of the block to add greater precision to the results. The results are again passed along from block to block in the same manner. The symmetry between Up and Down blocks is purposeful.[20]

3 Related Works

The topics of derived bathymetry and coastline detection are not new, and a great amount of valuable research exists on the topics and different implementations of the two subjects. The basis for these methods relies on older methods or provide a more limited scope of assessment than this paper.

Peter Etnoyer put forth a paper in 2005 outlining a comparison between satellite derived global relief data to echosounder-derived multibeam survey values in the Gulf of Alaska. Using existing data, the paper found that positioning of the sea mounts in the derived relief data was generally consistent with existing bathymetric survey data. However, the seamounts explored typically varied in depth by 192 meters. The study also found that the cell size of the remotely sensed data directly impacted the accuracy of the relief and whether the seamounts were detected. The study suggests using higher resolution imagery for the relief creation to alleviate the cell size issue. [1]

At the 2013 Hydro International Conference a team from the University of New Hampshire, led by Shachak Pe'eri, presented their findings from a study performed using LANDSAT imagery and existing derived bathymetry algorithms to map shallow water. They found that the process holds merit for the purpose of reconnaissance as the end product did not meet current mapping and charting criteria in accordance with the IHO S-55 and S-44 standards. These issues are caused by the large cell size of LANDSAT imagery. [2]

Two groups in 2008 and 2010 researched the use of coastline change detection using remotely sensed data. Ali Asghar Alesheikh, et al exams common techniques using remotely sensed data and creates a new technique merging those to detect changes in coastline. This new technique uses histogram thresholding and band ratio analysis. [4] Xuejie Li et al, uses similar techniques combined with ground truthing to evaluate the changes of coastline in the Pearl River Estuary in China. Using traditional techniques and sediment plume distribution the study determined large areas of coastal change that will impact human development in the area. [5]

A study on machine learning analysis for mapping land-cover was performed by John Rogan et al and utilized two classification trees and an artificial neural network. The study evaluated the performance of the machine learning approaches by evaluating accuracy, sensitivity, and resistance to training data deficiencies. The study found that the neural network created a change map most like one a human would generate. [3]

Machine learning and remotely sensed data appear in a study by Yun-Jae Choung et al in 2017. This study uses remotely sensed data and compares two methods, a water column method used in surveying and a support vector machine algorithm. The two methods were compared and the SVM method was found more accurate in producing a coastline where the plane between hydrosphere and lithosphere is well-defined. Both processes performed poorly in areas where the separation between land and water was less defined. [6]

Yun-Jae Choung's research is similar in nature to that of Zhang Hannv, Jiang Qigang, and Xu Jiang in 2013. In their paper they apply a SVM model for feature extraction and classification to LandSat7 data to extract coastline. They then use this data to modify existing coastline data within the framework of a GIS system. Unlike

previously cited research they attempt to adjust the algorithm for different coastline features such as sandy, rocky, or mangrove to create an accurate coastline and define characteristics of the coastline for analysis purposes. [7]

Predicting bathymetry values from remotely sensed imagery using machine learning processes Haibin Su et al. used a regression-kriging technique to predict bathymetric values. They developed an interpolated surface using their regression-kriging technique and compared specific points to the interpolated surface where ground-truth existed. This met with broad success and increased accuracy compared to the previous log-linear models standard at the time. [19]

In recent years many researchers have focused on the use of machine learning algorithms for the purpose of feature classification useful for coastline detection. Several studies used deep learning for feature classification on imagery such as Yongyang Zu et. al. who utilized CNNs to classify buildings in remotely sensed imagery. This process used semantic segmentation via a CNN in order to separate buildings from everything else, or clutter [14]. Ruirui Li et al developed a deep fully convolutional network with symmetrical up and down blocks called DeepUNet for the purpose of sea-land segmentation. This algorithm builds off older structures like SeNet and U-Net and modifies them to include edge detection algorithms. The results prove highly accurate compared to older models [20].

More researchers are beginning to pay attention to the importance of the hydrographic realm when looking at machine learning. Shan Liu et al developed a use for an BPANN to estimate bathymetric depths by introducing localization factors to the BPANN. This occurs by adjusting weights the further the a depth prediction is made from the ground truth points. The results increase accuracy over traditional regression methods [15]. Omar Makboul et al developed a traditional ANN model for estimating depths from remotely sensed data near Alexandria, Egypt. The accuracy of which is lower than the previous study but still provide a greater accuracy and confidence level than older regression methods. [17]

The previous studies lay an impressive groundwork for evaluating the usefulness of deep learning techniques for the purpose of bathymetry estimate prediction and coastline feature classification. Previous studies examined the use of SVM and other classification techniques for coastline feature extraction. The use of neural networks was examined for terrestrial land-cover mapping as well as hydrographic implementations. This study will seek to differentiate itself by modifying the DeepUnet for coastline detection and using RNN for bathymetric prediction.

4 Data

4.1 Data Selection

The training and test data used for both the derived bathymetry and coastline sections of the study consists of 376 multispectral images collected from the Orbview-3 satellite and downloaded from the USGS EarthExplorer API an example can be seen in figure 7. Only images with less than 10% cloud cover were selected, as cloud cover can provide a confounding factor when performing analysis.

The sensor collected the images between 2005 and 2007 and focus on the region of the Pacific covering Micronesia, the Mariana Islands, Marshall Islands, Guam, and Wake Island. The Orbview-3 platform collected multispectral imagery at the 4 meter resolution and the images are orthorectified, or projected, to the World Geodetic System 1984 (WGS1984) datum.[9] Multispectral bands range from 450 to 900 nm wavelengths which comprise the blue, green, red, and near infrared bands. The spatial resolution is 1 meter by 1 meter pixels and the swath width of the images covers a range of 8 kilometers.

This region of the world was selected for analysis due to the low turbidity and clearness of the water. Remotely sensed data under ideal conditions can only penetrate roughly 30 meters of water depth, and the Pacific islands have clear water, low turbidity, and still contain a wide variety of coastlines and bathymetric features to make training a model possible.

To verify depth predictions and coastline detection, existing nautical charts from the National Oceanic and Atmospheric Administration (NOAA), UKHO, and international charts are utilized. These charts exist in a digital format orthorectified in WGS1984. The sounding information on the charts will be compared to the derived depths output by the deep learning model in a visual comparison.

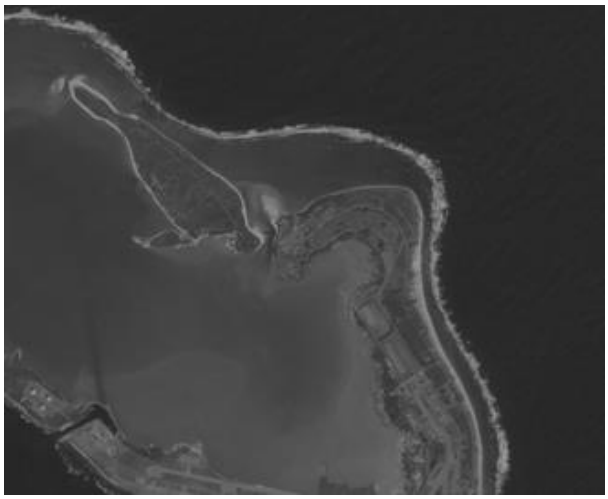

Figure 7. Example Image from OrbView-3

5 Methods

5.1 Data Preparation

The first step of data preparation involves resizing the images to the same size and aspect ratio and aligning the band channels of the multispectral imagery. This

[9] Orbview-3 [Online] https://space.skyrocket.de/doc_sdat/orbview-3.htm [Accessed 4 November 2018]

ensures that no shifts between images exist. To combat the small sample size and to allow for limited processing power, the images are cropped into 640x640 pixel tiles. Only tiles that contain a sea-land boundary are used in this analysis. This expands the original limited set of remotely sensed images to 27,785 samples. Next, the images are normalized to create a standard range for each channel of each pixel.

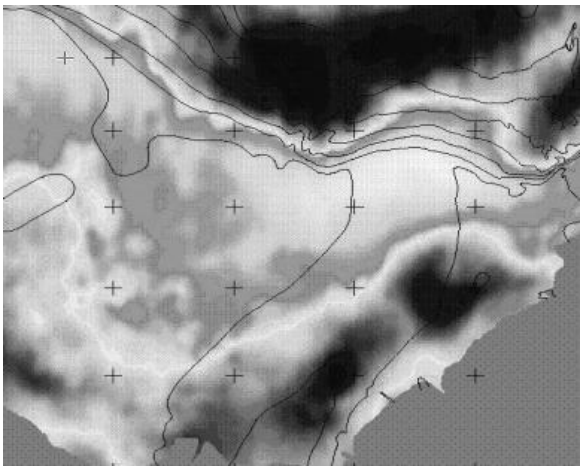

Figure 8. Interpolated depths from nautical chart soundings.

Ground truth data is generated from the nautical charts by interpolating a depth surface from the depth values, as in the example interpolation shown in figure 8. These values are augmented by hazard depths where available. The interpolated surfaces are not ideal for this analysis but are the only source of bathymetric data readily available to the public. Interpolated data is not ideal since that means the test data predictions will be compared to estimations rather than actual ground truth, excepting the control points for the interpolation.

5.2 Building the Models

The basic structure of the models used will come from existing models for seafloor segmentation or sea-land segmentation neural networks. The bathymetric deep learning model will use an RNN structure while the coastline model will utilize the DeepUNet CNN model. These will be modified to attempt to create more accurate results, increase output resolution, and decrease processing time.

5.3 Bathymetric RNN Construction

For bathymetric modeling, a RNN was chosen, because sounding depths usually are found near other sounding depths of like values. The seafloor can be considered a continuous surface where any changes in the seafloor occur over a wider area. While isolated depths and shoals exist, they are an exception.

The core structure of the bathymetric RNN remains the same for a simple RNN. The RNN uses a masked convolution to split each pixel input into three layers, one each for the RBG bands. The connections between nodes in these layers are

weighted with the sum of all outputs from the previous layer. A function is applied and these weights plus the initial value is passed onto the next node. In this way, the context of the pixel is preserved, and each node learns from the previous.

5.4 Coastline Modified DeepUNet CNN Construction

The modifications performed in this study will break the symmetry to maximize accuracy while decreasing the distortion from the original input. Figure 9 details the specific modifications used in this study. The kernel size remains the same for each convolutional layer in the upblock, 3x3 as do the kernel size of 64 and 32.

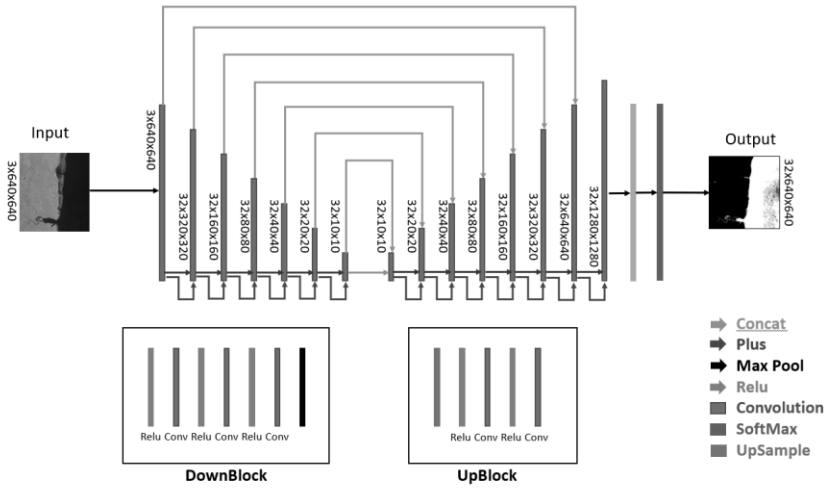

Figure 9. Modified DeepUNet Structure

In order to accomplish these goals two changes are made. An additional convolution layer is added to each of the down blocks in the hopes that it will increase the accuracy of the result passed via the maxpooling layer to the next block. Breaking the asymmetry of DeepUNet, an additional up block is added at the tail end with a final size of 1280 pixels. This allows the SoftMax layer to reduce the size and end up with an output image of equal pixel size to the input with minimal distortion and artifacts.

5.5 Training the Models

Training of the Bathymetric RNN consist of 100 epochs with a backpropagation of 12 pixels. This is executed on the derived images from the original 376 images. At the end of training measures of fit are calculated using a mixture of the different RBG bands of the image. Table 2 shows that the R^2 doesn't look very impressive at this point, but the data may also not be linear in relationship either. The best R^2 seems to occur when using the red and blue bands (3 and 2 respectively). However, the differences between bands looks marginal.

Table 2. Bathymetry RNN Measures of Fit

Measures of Fit		
Bands	**R2**	**RMSE**
Green, Red	0.691	0.884
Green	0.699	0.814
Blue, Green	0.697	0.876

Training for the coastline CNN consists of 1000 epochs of the 376 images. GPU processing power was utilized to speed up the processing from simply using the CPU as well as to accommodate the larger than usual tile size for this study. A learning rate of 0.1 is selected initially. This is adjusted downward to 0.05 once half the samples are processed. The momentum for this model was set high at 0.9.

The overall accuracy of the model over several epochs is shown in figure 10 while the loss is shown in figure 11. These show a lower than expected initial accuracy but otherwise follow a standard training pattern given the momentum and learning rate used. The expected accuracy was nearer to the DeepUNet accuracy while the actual overall accuracy of the model reached 95.41%.

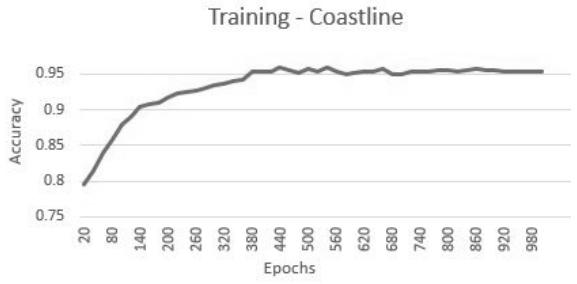

Figure 10. Accuracy of DeepUNet Modifications over Epochs

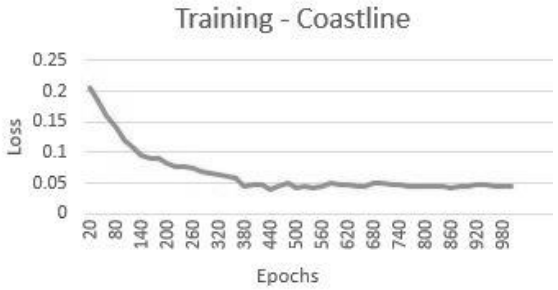

Figure 11. Loss of DeepUNet Modifications Over Epochs

6 Results

6.1 Derived Bathymetry Results

This section contains the final output results of the bathymetric prediction RNN model. It also discusses the verification of the results by comparing to modern nautical charts as well as calculating the Mean Absolute Error (MAE) in meters to compare to the IHO standards for vertical accuracy.

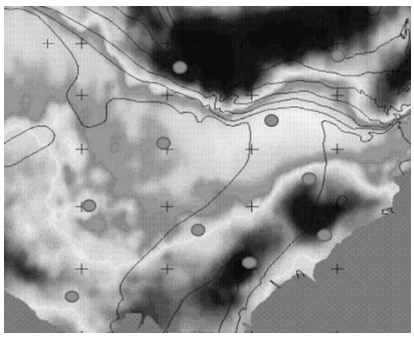

Figure 12. Derived Bathymetry Grid with Ground Truth Points

The result of the RNN for derived bathymetry creates a heat map of depth predictions, as shown in Figure 12. The heat maps can be compared to existing digital nautical data or, as in the case of this study, reviewed using digital charts. Known depths from hydrographic charts are compared to the depths predicted by the RNN, a sample of such appear in Table 3.

Table 3. Bathymetry Known Depth vs. Predicted

Bathymetry		
Site	**Known Depth**	**RNN Depth**
1	14.4m	13.53m
2	10.2m	8.4m
3	5.1m	8.07m
4	10.8m	13.82m
5	15.3m	13.28m
6	5.7m	8.51m
7	10.5m	9.74m
8	19.1m	14.12m
9	24.3m	22.51m
10	32m	35.94m

From this data, the residuals are calculated, and the MAE in meters of total vertical uncertainty is obtained. Depths from 1200 sounding points are used to evaluate the MAE with the result being 3.216 meters. This fails to meet the IHO specifications of 0.5 meters for category 1a and 1b surveys by a wide margin (Table 1).

6.2 Coastline Detection Results

This section contains the final output results of the coastline detection model, including the verification of the results by comparing to modern nautical charts as well as looking at error and loss results for the model after processing.

Figure 13. Modified DeepUNet Output

Final binary feature maps from the modified DeepUNet model are a binary white and black image, an example of which is figure 13. This is similar to the output generated from a thresholding process. In these images the white section represents water while the black represents the land. This result is compared to digital coastline data. Even without comparing to the ground truth data, several issues can be seen in figure 12, such as the artifacts on the right side of the feature map and the water that appears inland.

Figure 14 shows a transparent raster nautical chart superimposed on the binary feature map. In addition to the artifacts circled on the right and the inland water, several errors appear. In the uppermost portion of the image, the feature map appears to detect coastline further out to sea than shown on the chart. This is likely due to the imagery taken at a timeframe closer to low-tide, and some of the intertidal zone is captured as coastline. The middle circle also appears to show the same issue but the DeepUNet did pick up the natural channel inland with high accuracy.

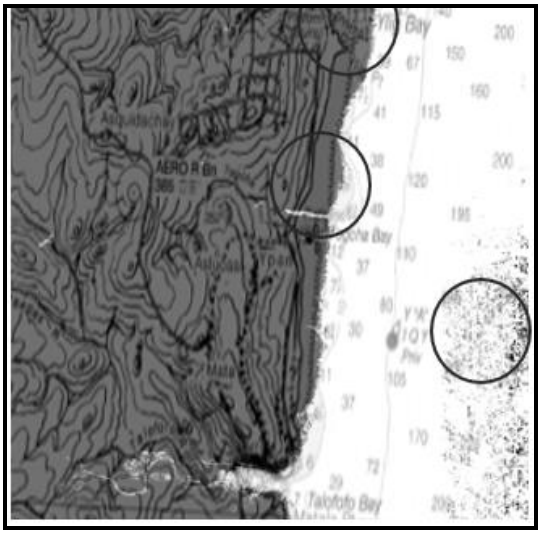

Figure 14. Coastline Output Overlayed with Raster Chart

Over all 376 images, the results of the modified DeepUNet appear to fall short of DeepUNet. Table 4 shows the evaluation metrics for the modified DeepUNet. While all of these metrics are positive, the overall precision and recall of DeepUNet are both 99.04% [20]. This is likely the result of artifacts being introduced into the system with the additional upsampling block.

Table 4. Modified DeepUNet Coastline Model Metrics

Model	Precision	F1	Recall
Modified DeepUNet	95.41%	94.20%	92.12%
DeepUNet	99.04%	98.71%	99.04%

6.3 Comparison to Previous Studies

This section contains a comparison of the modified DeepUNet for coastline detection presented in this paper with the SVM model used in the Dejan Vukadinov, Raka Jovanovic, and Milan Tuba report [10] and the original DeepUNet model [20]. An analysis of the differences between the results of each as well as the potential benefits of both models will be presented. Finally, a look at the stumbling blocks for each model will also be considered.

Table 5. Comparative Accuracy of Coastline Detection Methods

Overall Precision			
Modified DeepUNet	**DeepUNet**	**SVM**	**Regression**
95.41%	99.04%	80.72%	88.40%

Deep learning models clearly outpace other machine learning methods and traditional regression methods for determining coastline. Table 5 shows that while the original DeepUNet stands as the most precise method, the modified deep learning model follows closely behind. Support vector Machines performed poorest of all methods but that is partially accounted for in the study as issues correcting for coastline type (rocky, sandy, etc) [10]. While the modified DeepUNet showed less precise results than DeepUNet, this lends clear evidence that deep learning models for coastline detection and derived bathymetry should be explored.

7 Ethical Considerations

The use of derived bathymetry and coastline change detection via remotely sensed imagery is not without ethical considerations. Formal bathymetric surveys typically occur in territorial waters and with the permission of the host country. Often, this permission comes with the request that survey findings are not made publicly available and the host country receives a copy of the data. Many countries are remiss to provide access to territorial waters to foreign entities understanding that bathymetric survey information could be used by militaries to aid subsurface navigation by military vessels.

While coastline detection's primary purpose involves safety of navigation and humanitarian aid in the unfortunate case of a natural disaster or other crisis, it too can be utilized for military purposes. Coastline plays an important role in amphibious operations. Typically, coastline is surveyed in a similar manner to bathymetry via an official survey of record, and - if performed by a foreign power, they must receive permission from the host country. Using remotely sensed data to determine the coastline circumvents that process as the data is generated from satellites or other remote sensors.

Malicious state actors utilize derived bathymetry to lay claim and expand influence in areas of the ocean where no land exists. A derived bathymetric dataset could be utilized to determine areas such reefs, atolls, and shoals that can be built upon to create artificial islands and make claims of territorial waters and exclusive economic zone. While derived bathymetry was not used in existing cases, the buildup of shallow water by states seeking to expand their influence is a great worry in many regions of the world and derived bathymetry could play a role in both expanding or refuting this practice.

8 Conclusions

The results of this study show modest accuracy results in predicting depths with a RNN. The accuracy decreases as the depths increase, although this is expected as confounding factors such as turbidity, salinity, and seafloor composition can confound sensors. The accuracy from this process does not meet the criteria for an IHO category 1a survey for vertical accuracy, and thus, the data should not be used to supplement actual safety of navigation products.

The modification of the DeepUNet CNN model added two additional components to the up-sampling and down-sampling blocks. The results were a slight drop in accuracy but a higher resolution of the output image. This traded some accuracy for a higher resolution output. This also led to greater processing times though, so the additions may not ultimately be worthwhile due to artifacts and inconsistencies with the output. The use of this coastline for safety of navigation products is not recommended.

The intent behind this study was not to replace or augment actual safety of navigation products, but to rather inform decision makers of where significant divergence exists between the modelled data and existing charted data. This allows valuable resources to be allocated towards the most critical areas. The outputs of these bathymetric predictions and coastline detection models can be used to detect areas of significant change in unexpected areas and can be used to check the veracity of existing data. The use of deep learning to predict bathymetric depths and detect coastline allows for the effective deployment of valuable and limited survey resources to ground truth the most critical areas for maritime safety of navigation.

9 Future Work

This study compared derived bathymetry to existing nautical charting products due to limitations on resources and publicly available data. Additional research should include the comparison of derived bathymetric outputs from the neural networks with more robust survey data in the form of bathymetric attribute grids, the standard output of most modern multi-beam surveys. This could provide a pixel by pixel comparison of the derived bathymetry for better accuracy and error rates and would likely lead to better models. Additional information could be integrated into the model in order to properly identify specific features such as hazardous rocks and the model can be adjusted to determine the bottom characteristics of the seafloor.

Additional work on the coastline detection could focus on combining other sensors in order to more accurately depict coastlines. Single aperture radar provides a great method for separating water from other landforms as water has high absorption of radio wavelengths and water shows up distinctly black compared to other landforms that reflect higher levels of radio waves. This could be combined with multispectral imagery to highly define the water area while the multispectral imagery better defines the actual land boundary. Ideally more recent remotely sensed data would be utilized to determine change between charted and actual coastline. This study uses older data due to availability.

One of the key issues with using remotely sensed data to observe oceans are the effects of tides on the results. Safety of Navigation products rely on a safety margin and thus they use depths taken at the lowest astronomical tide (LAT) for a given area. This holds especially true the closer the depths move towards land. Similarly, coastline typically refers to the highest tide marker with the area between lowest tide and highest tide known as the intertidal region. As such, remotely sensed imagery should account for the precise time of LAT in order to properly predict depths while taken at high tide to detect the appropriate coastline. This study did not factor in the time the imagery was taken or the tides in these regions. This likely played a role in lowering the overall accuracy of the results.

References

1. Etnoyer, P. (2005), Seamount resolution in satellite-derived bathymetry, Geochem. Geophys. Geosyst., 6, Q03004.

2. Pe'eri, Shachak; Azuike, Chukwuma; and Parrish, Christopher, "Satellite-Derived Bathymetry a Reconnaissance Tool for Hydrography" (2013). Hydro International. 1119.

3. Rogan, J., Franklin, J., Stow, D., Miller, J., Woodcock, C., & Roberts, D. (2008). Mapping land-cover modifications over large areas: A comparison of machine learning algorithms. Remote Sensing of Environment, 112(5), 2272-2283.

4. Alesheikh, A.A., Ghorbanali, A., Nouri, N., (2007). Coastline change detection using remote sensing. Int. J. Environ. Sci. Tech., 4 (1), 61-66.

5. Li, X., & Damen, M. C. (2010). Coastline change detection with satellite remote sensing for environmental management of the Pearl River Estuary, China. Journal of Marine Systems, 82.

6. Yun-Jae Choung and Myung-Hee Jo, Comparison between a Machine-Learning-Based Method and a Water-Index-Based Method for Shoreline Mapping Using a High-Resolution Satellite Image Acquired in Hwado Island, South Korea, Journal of Sensors, vol. 2017.

7. Hannv, Z., Qigang, J., & Jiang, X. (2013). Coastline Extraction Using Support Vector Machine from Remote Sensing Image. Journal of Multimedia, 8(2), 175-182

8. Lyzenga, D., Malinas, N., & Tanis, F. (2006). Multispectral bathymetry using a simple physically based algorithm. IEEE Transactions on Geoscience and Remote Sensing, 44(8), 2251-2259.

9. Stumpf, R. P., Holderied, K., & Sinclair, M. (2003). Determination of water depth with high-resolution satellite imagery over variable bottom types. Limnology and Oceanography, 48, 547-556.

10. Dejan, Vukadinov, Raka, Jovanovic, Milan, Tuba. (2017) An Algorithm for Coastline Extraction from Satellite Imagery. International Journal of Computers, 2, 8-15.

11. Schmidhuber, J. (2015). Deep learning in neural networks: An overview. Neural Networks, 61, 85-117.

12. IHO standards for hydrographic surveys (Edition 5). (2008). Monaco: International Hydrographic Bureau.

13. Aqeel, M., Jamil, M., & Yusoff, I. (2011). Introduction to Remote Sensing of Biomass. *Biomass and Remote Sensing of Biomass*.

14. Xu, Y., Wu, L., Xie, Z., & Chen, Z. (2018). Building Extraction in Very High Resolution Remote Sensing Imagery Using Deep Learning and Guided Filters. *Remote Sensing,10*(1), 144.

15. Liu, S., Wang, L., Liu, H., Su, H., Li, X., & Zheng, W. (2018). Deriving Bathymetry From Optical Images With a Localized Neural Network Algorithm. *IEEE Transactions on Geoscience and Remote Sensing,56*(9), 5334-5342.

16. Xu, N. (2018). Detecting Coastline Change with All Available Landsat Data over 1986–2015: A Case Study for the State of Texas, USA. *Atmosphere,9*(3), 107.

17. Makboul, O., Negm, A., Mesbah, S., & Mohasseb, M. (2017). Performance Assessment of ANN in Estimating Remotely Sensed Extracted Bathymetry.

Case Study: Eastern Harbor of Alexandria. *Procedia Engineering,181*, 912-919.

18. Gholamalifard, M., Kutser, T., Esmaili-Sari, A., Abkar, A., & Naimi, B. (2013). Remotely Sensed Empirical Modeling of Bathymetry in the Southeastern Caspian Sea. *Remote Sensing,5*(6), 2746-2762.

19. Su, H., Liu, H., & Wu, Q. (2015). Prediction of Water Depth From Multispectral Satellite Imagery—The Regression Kriging Alternative. *IEEE Geoscience and Remote Sensing Letters,12*(12), 2511-2515.

20. Li, R., Liu, W., Yang, L., Sun, S., Hu, W., Zhang, F., & Li, W. (2018). DeepUNet: A Deep Fully Convolutional Network for Pixel-Level Sea-Land Segmentation. *IEEE Journal of Selected Topics in Applied Earth Observations and Remote Sensing,11*(11), 3954-3962.